Title	Miniaturized dual-band bandpass filter using λ/2 spiral-resonator and loaded open-stub
Author(s)	Luo, X; Sun, S; Li, E
Citation	The 2012 IEEE International Microwave Symposium (MTT-S), Montreal, QC., 17-22 June 2012. In IEEE - MTTS International Microwave Symposium Digest, 2012
Issued Date	2012
URL	http://hdl.handle.net/10722/165300
Rights	IEEE - MTTS International Microwave Symposium Digest. Copyright © IEEE.

Miniaturized Dual-Band Bandpass Filter Using $\lambda/2$ Spiral-Resonator and Loaded Open-Stub

Xun Luo [1,2], Sheng Sun [3], and Er-Ping Li [4]

[1]Huawei Technologies Co., Ltd., Shenzhen, 518129, China
[2]Univerisity of Electronic Science & Technologies, Chengdu, 610054, China
[3]The University of Hong Kong, Hongkong, China
[4]A*star, Institute of High Performance Computing, 138632, Singapore

***Abstract*— In this paper, a miniaturized dual-band bandpass filter using the half-wavelength ($\lambda/2$) spiral-resonators and loaded open-stubs with a spiral-coupled scheme is proposed. The mechanism of the dual-band operation is shown as follows. The first passband resonance is employed by the fundamental resonant-mode (i.e., f_1) of the $\lambda/2$ spiral-resonator. Meanwhile, the loading effect introduced by the loaded open-stub could shift the first-spurious (i.e., f_2) of the $\lambda/2$ spiral-resonator downward, which leads to a finely adjusted second passband resonance. Then, based on the $\lambda/2$ spiral-resonators with loaded open-stubs mentioned above, the spiral-coupled scheme is implemented, which employs a strong enough passband enhancement around the dual-resonances to achieve the dual-band bandpass filter. Besides, the loaded-tapping scheme could produce five transmission zeros, which can not only enhance the dual-band passband selectivity, but also extend the upper stopband bandwidth with a good rejection level. To verify the mechanism above, a dual-band bandpass filter operated at 1.035 and 1.56 GHz is designed, implemented, and fabricated. A good agreement between the simulation and measurement is achieved.**

***Index Terms*— Bandpass filter, dual-band, spiral-resonator, loaded open-stub, spiral-coupled scheme.**

I. Introduction

Dual-band bandpass filter is one of the critical key components in the dual-band wireless communication system. Therefore, various structures have been developed to meet the ever-increasing practical application limits [1]-[10]. The dual-mode ring resonator with a compact size and easily adjusted dual-resonances has been widely employed for the dual-band bandpass filter design [2]-[4] with a relatively narrow upper stopband. To extend the upper stopband bandwidth of the dual-band bandpass filter, the stepped-impedance resonator (SIR) has been employed [5]-[8]. However, the sizes of these filters are relatively large. Recently, the embedded spiral resonator (ESR) [9], comb-loaded resonator [10], and circular cavity [11] are introduced to implement filters with good dual-band frequency responses. Nevertheless, the design of dual-band bandpass filter with good passband selectivity, wide stopband, and a compact size remains challenging.

In this paper, a dual-band bandpass filter with a competitive size is proposed. The bandpass filter consists of two half-wavelength ($\lambda/2$) spiral-resonators with loaded open-stubs, which are implemented with a spiral-coupled scheme. The dual-resonances (i.e., f_1 and f_2) are introduced by the $\lambda/2$ spiral-resonators with a loaded open-stub. Meanwhile, the spiral-coupled scheme is employed to achieve strong passband enhancement around the f_1 and f_2. Besides, five transmission zeros can be afforded by the loaded-tapping scheme, which can not only improve the passband selectivity, but also extend the upper stopband bandwidth with a good rejection level. The proposed filter with good frequency responses has a compact size as 35.96 mm × 18 mm (i.e., 0.160 λ_g × 0.084 λ_g, where λ_g is the microstrip guided wavelength on the substrate at the center frequency of 1.035 GHz).

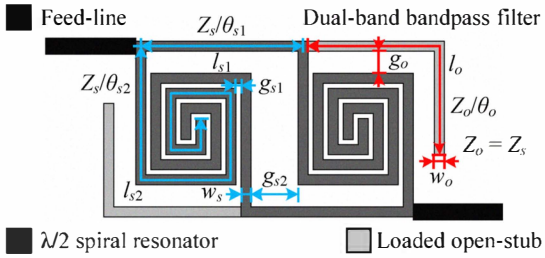

Fig. 1. Layout of the proposed dual-band bandpass filter.

II. Schematic and Operation

Fig. 1 shows the layout of the dual-band bandpass filter. The filter consists of two $\lambda/2$ spiral-resonators (i.e., Z_s/θ_s, where $\theta_s = \theta_{s1} + 2\theta_{s2}$) with loaded open-stubs (i.e., Z_o/θ_o, $Z_o = Z_s$), which are implemented as a spiral-coupled scheme [1]. Besides, to excite the filter, two 50Ω feed-lines are directly tapped to the $\lambda/2$ spiral-resonators, acting as the input/output (I/O) ports. To investigate the mechanism of the proposed scheme, the EM simulator IE3D and RT/5880 dielectric substrate with ϵ_r of 2.2 and a thickness of 0.508 mm are used.

A. $\lambda/2$ Spiral-Resonator with Loaded Open-Stub

Fig. 2 depicts the simulated dual-resonances (i.e., f_1 and f_2) current density distribution of the $\lambda/2$ spiral-resonator with a loaded open-stub. As illustrated in Fig. 2(a), it is notable that the strong current density is distributed on the $\lambda/2$ spiral-resonators, which can allocate the f_1. Thus, from the resonant condition, the f_1 can be derived as

$$f_1 = \frac{c}{2\left(l_{s1} + 2l_{s2}\right)\sqrt{\epsilon_{eff}}} \tag{1}$$

978-1-4673-1088-8/12/$31.00 ©2012 IEEE

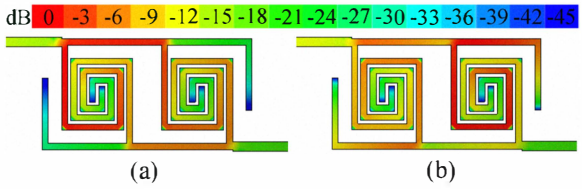

Fig. 2. Simulated dual-resonances current density distribution of the proposed scheme. (a) First resonance f_1. (b) Second resonance f_2.

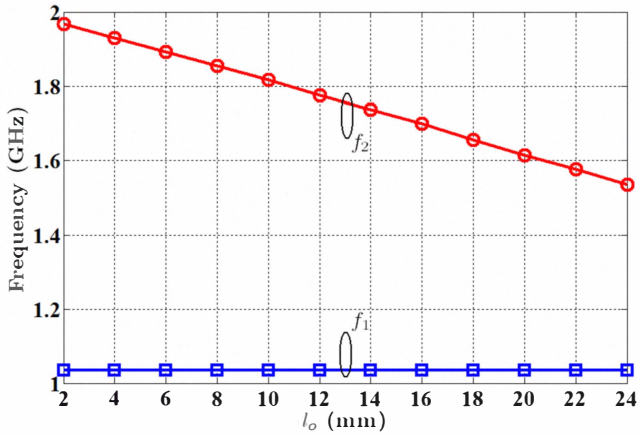

Fig. 3. The effect of the loaded open-stub (i.e., length l_o) on the f_2. (l_{s1} = 16.12 mm and l_{s2} = 47.74 mm.)

where $l_{s1} + 2l_{s2}$ is the physical length of the $\lambda/2$ spiral-resonator, c is the velocity of the light in free space, and ϵ_{eff} is the efficient dielectric constant of the substrate. Besides, it can be seen that the current density is mainly concentrated on the $\lambda/2$ spiral-resonator and loaded open-stub, as depicted in Fig. 2(b). This means that the strong loading effect of the loaded open-stub could shift the first spurious f_2 of the $\lambda/2$ spiral-resonator downward, as shown in Fig. 3. It is seen that once the length l_o of the loaded open-stub increases, the f_2 decreases. However, the variation of the l_o has no effect on the f_1. Thus, it can be concluded that once the specific f_1 is fixed (i.e., the physical dimensions l_{s1} and l_{s2} are determined), the f_2 can be adjusted with a wide range by the loaded open-stub to meet the requirement of the dual-band operation.

B. Spiral-Coupled Scheme

The spiral-coupled scheme can afford strong enough pass-band enhancement around the dual-resonances (i.e., f_1 and f_2) [12]. As depicted in Fig. 2, it can be seen that the electric current density of the spiral-lines has an uniform concentration at the resonances. By making the width w_s wider and gap g_{s1} narrower, a smoother current distribution can be obtained. Therefore, the quality factor of the resonator could be improved with less conductor loss. As such, the ratio of the width w_s to gap g_{s1} in the $\lambda/2$ spiral-resonator is optimized and chosen as 2:1. Fig. 4 shows the loss responses of the proposed scheme. It can be seen that the conductor loss of the structure in both passbands is less than 0.155, which will lead to the competitively low passband insertion loss comparing to

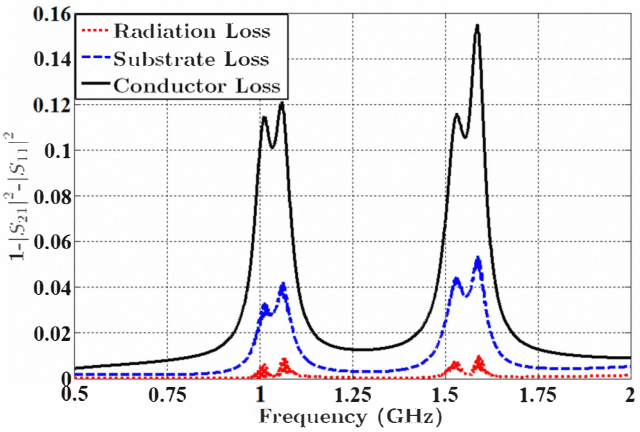

Fig. 4. Simulated loss factors of the spiral-coupled scheme against frequency. (Dotted line: radiation loss; Dashed line: substrate loss; Solid line: conductor loss.)

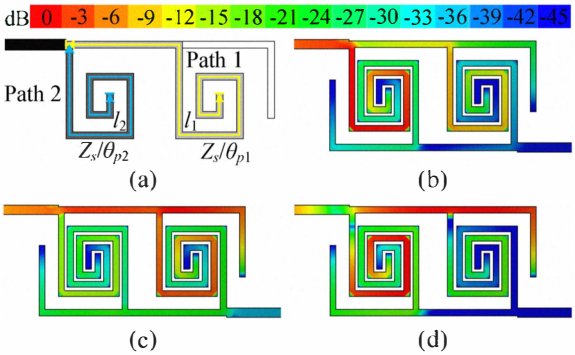

Fig. 5. (a) Paths of the transmission zeros f_{z1} and f_{z2}. (b) Simulated current density distribution of the f_{z3}. (c) Simulated current density distribution of the f_{z4}. (d) Simulated current density distribution of the f_{z5}.

the patch scheme with low loss responses [13].

C. Loaded-Tapping Scheme

As shown in Fig. 5, the location of the tapped feed-line can determine the paths to allocate the transmission zeros (i.e., f_{z1} and f_{z2}) around the first-resonance f_1, which enhance the first passband selectivity. The mechanism is studied as follow. The input equivalent admittances Y_{ink} (k = 1 and 2) viewed from the tapping position to the open ends could be generated and calculated as

$$Y_{ink} = -jY_s \tan \beta l_k \tag{2}$$

where Y_s is the characteristic admittances of the paths, and l_k (k = 1 and 2) is physical lengths of path k, respectively. Note that, the transmission zeros (i.e., f_{z1} and f_{z2}) can be finely tuned while the electric lengths of each path correspond to a quarter-wavelength [1]. Meanwhile, as shown in Fig. 5(b), the current is distributed on the path 1 and path 2 of the upper $\lambda/2$ spiral-resonator with a loaded open-stub. This means resonance occurs and the signal can not pass through it. Therefore, the transmission zero f_{z3} is allocated when the

978-1-4673-1088-8/12/$31.00 ©2012 IEEE

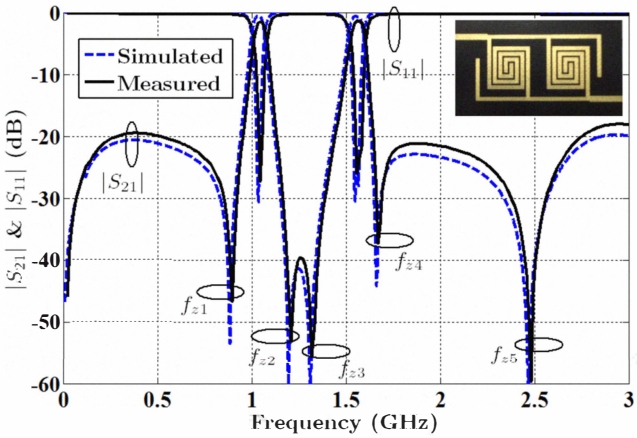

Fig. 6. Measured and simulated results of the dual-band bandpass filter. (g_o = 2.16 mm, g_{s1} = 0.5 mm, g_{s2} = 4.62 mm, l_o = 24.1 mm, l_{s1} = 16.12 mm, l_{s2} = 47.74 mm, and $w_o = w_s$ = 1 mm.)

total admittance of two paths at f_{z3} is zero [14] as follow

$$Y_{in1} + Y_{in2} = 0 \tag{3}$$

As depicted in Fig. 5(c) and (d), it can be concluded that the mechanism to generate the f_{z4} and f_{z5} is similar as the f_{z3}, and thus it is not repeated here. Note that f_{z3} and f_{z4} are employed to improve the second passband selectivity, and the f_{z5} is introduced to extend the upper stopband bandwidth with a good rejection level.

D. Filter Design

The design procedure of the dual-band bandpass filter is shown as follows. The first step is to determine the first- and second-resonances (i.e., f_1 and f_2) of the dual-passbands. The f_1 could be properly adjusted by the $\lambda/2$ spiral-resonator, while the length (i.e., l_{s1} + $2l_{s2}$) is chosen as 180 degrees at f_1. Meanwhile, the specific f_2 can be achieved by tuning the size (i.e., l_o) of the loaded open-stub, once the f_1 is fixed. The second step is to obtain the quality factors to meet the dual-bands limits. It is found that good quality factors with low conductor loss can be achieved, while the ratio of the width w_s to gap g_{s1} in the $\lambda/2$ spiral-resonator is chosen as 2:1. The third step is to determine the size of the coupling structure to satisfy the requirement of the coupling coefficients (i.e., k_L and k_U) for both passbands. In order to realize the desired values for k_L and k_U, the pole-splitting method [1] in conjunction with full-wave simulations are employed. It is found that the gaps g_{s2} and g_o are the critical elements to dominate the k_L and k_U, respectively. So far, the initial dimensions of the proposed filter can be obtained, and the fine tuning can be carried out to meet the practical specifications.

Based on the procedures above, a dual-band bandpass filter at 1.035 and 1.56 GHz is designed and fabricated. The measurement is performed using Agilent 5230A network analyzer. As shown in Fig. 6, the filter exhibits the insertion loss less than 1.39 dB, including the loss from the SMA I/O ports (i.e., 0.7 dB in both passbands), and the return loss better than 20 dB in both passbands, respectively. Besides, the filter can generate five transmission zeros (0.887, 1.198, 1.313, 1.666, and 2.469 GHz) in the stopband, which provide the wide stopband with a good rejection level and much improved passband selectivity. In addition, the proposed filter exhibits a compact circuit size as 35.96 mm × 18 mm (i.e., 0.160 λ_g × 0.084 λ_g, where λ_g is the microstrip guided wavelength on the substrate at the center frequency of 1.035 GHz).

III. Conclusion

In this paper, a compact dual-band bandpass filter is proposed based on the $\lambda/2$ spiral-resonators with loaded open-stubs, which can employ the finely adjusted dual-resonances. Meanwhile, the spiral-coupled scheme can introduce the strong enough dual-band passband enhancement around the dual-resonances. Besides, five transmission zeros are employed by the loaded-tapping scheme. These transmission zeros can not only improve the passband selectivity, but also extend the stopband bandwidth with a good rejection level. With good frequency performance and a compact size, the proposed filter is attractive to the dual-band wireless applications.

References

[1] J.-S. Hong and M. J. Lancaster, *Microstrip Filters for RF/Microwave Applications*, New York: Wiley, 2001.

[2] Y.-C. Chiou, C.-Y. Wu, and J.-T. Kuo, "New miniaturized dual-mode dual-band ring resonator bandpass filter with microwave C-sections," *IEEE Microw. Wireless Compon. Lett.*, vol. 20, no. 2, pp. 67–69, Feb. 2010.

[3] S. Sun, "A dual-band bandpass filter using a single dual-mode ring resonator," *IEEE Microw. Wireless Compon. Lett.*, vol. 21, no. 6, pp. 298–300, Jun. 2011.

[4] Y. C. Li, H. Wong, and Q. Xue, "Dual-mode dual-band bandpass filter based on a stub-loaded patch resonator," *IEEE Microw. Wireless Compon. Lett.*, vol. 21, no. 10, pp. 525–527, Oct. 2011.

[5] J.-T. Kuo, T.-H. Yeh, and C.-C. Yeh, "Design of microstrip bandpass filters with a dual-passband response," *IEEE Trans. Microw. Theory & Tech.*, vol. 53, no. 4, pp. 1331–1337, Jul. 2005.

[6] W.-S. Chang and C.-Y. Chang, "Analytical design of microstrip short-circuit terminated stepped-impedance resonator dual-band filters," *IEEE Trans. Microw. Theory & Tech.*, vol. 59, no. 7, pp. 1730–1739, Jul. 2011.

[7] R. Gómez-García, J.-M. Muñoz-Ferreras, and M. Sánchez-Renedo, "Signal-interference stepped-impedance-line microstrip filters and application to duplexers," *IEEE Microw. Wireless Compon. Lett.*, vol. 21, no. 8, pp. 421–423, Aug. 2011.

[8] C.-W. Tang and P.-H. Wu, "Design of a planar dual-band bandpass filter," *IEEE Microw. Wireless Compon. Lett.*, vol. 21, no. 7, pp. 362–364, Jul. 2011.

[9] X. Luo, H. Qian, J.-G. Ma, K. Ma, and K. S. Yeo, "Compact dual-band bandpass filters using novel embedded spiral resonator (ESR)," *IEEE Microw. Wireless Compon. Lett.*, vol. 20, no. 8, pp. 435–437, Aug. 2010.

[10] C.-W. Tang, Y.-K. Hsu, and J.-W. Wu, "Design of wide dual-passband microstrip bandpass filters with comb-loaded resonators," in *2010 IEEE MTT-S Int. Microw. Symp. Dig.*, pp. 1700–1703, May. 2010.

[11] H. M. Hizan, I. C. Hunter, and A. I. Abunjaileh, "Integrated dual-band radiating bandpass filter using dual-mode circular cavities," *IEEE Microw. Wireless Compon. Lett.*, vol. 21, no. 5, pp. 246–248, May. 2011.

[12] K. H. Tsai and C.-K. C. Tzuang, "Design and analysis of a high directivity directional coupler using synthetic coupled lines in CMOS technology," in *40th European Microwave Conf.*, pp. 1174–1177, Oct. 2010.

[13] S. Sun and W. Menzel, "Novel dual-mode balun bandpass filters using single cross-slotted patch resonator," *IEEE Microw. Wireless Compon. Lett.*, vol. 21, no. 8, pp. 415–417, Aug. 2011.

[14] X. Y. Zhang, J.-X. Chen, J. Shi, and Q. Xue, "High-selectivity dual-band bandpass filter using asymmetric stepped-impedance resonators," *Electron. Lett.*, vol. 45, no. 1, pp. 63–64, Jan. 2009.

978-1-4673-1088-8/12/$31.00 ©2012 IEEE